Survey of the Linear Theta Pinch Work in Garching+

E. Fünfer

IPP 1/7o August 1967

INSTITUT FÜR PLASMAPHYSIK

GARCHING BEI MÜNCHEN

INSTITUT FÜR PLASMAPHYSIK

GARCHING BEI MÜNCHEN

Survey of the Linear Theta Pinch Work in Garching[+]

E. Fünfer

IPP 1/7o August 1967

[+]Invited paper presented at the "American Physical Society Topical Conference on Pulsed High Density Plasmas" held at the Los Alamos Scientific Laboratory, Los Alamos, N.M., September 19 - 22, 1967

Die nachstehende Arbeit wurde im Rahmen des Vertrages zwischen dem Institut für Plasmaphysik GmbH und der Europäischen Atomgemeinschaft über die Zusammenarbeit auf dem Gebiete der Plasmaphysik durchgeführt.

IPP 1/7o E.Fünfer Survey of the Linear Theta Pinch Work in Garching

(in English)

Abstract

The main objectives are very hot, high β-plasmas, collisionless compression and turbulent heating, and M & S - experiments. Low filling densities down to $1o^{12}$ cm^{-3} are required and pre-ionization becomes a severe problem. Therefore three different methods were investigated: the high frequency theta pinch with dynamically confined plasma, the high-voltage z-pinch with short current pulse and the photoionization by strong ultraviolet radiation.

In the main discharge highly anisotropic plasmas with ion temperatures of several keV can be observed. The time behaviour of the anisotropy is compared with theoretical considerations.

Electron temperatures of some 1oo eV were found by laser scattering experiments. The values from X-ray absorption were much higher and not reproducible. Coherent laser scattering at $9o^{o}$ with a theta pinch of high density and low temperature allowed the measurement of spectrally resolved ion and satellite lines.

The influence of mirrors on end losses and stability has been studied. The plasma remains stable in the low pressure regime for a low impurity level.

Two-dimensional programmes are treated: a(r,z) programme for end losses and thermal conductivity and a(r, φ) programme for plasma rotation. A programme for collisionless compression with a phenomenological friction term was also treated.

A preliminary linear M & S - experiment (Limpus) on Isar I showed no noticeable difference in its behaviour as compared with a straight coil.

It is obvious that controlled fusion cannot be achieved with a linear theta pinch of reasonable length. One reason is end losses, which prevent a sufficiently long confinement time, even with mirrors. Consequently, some laboratories are planning toroidal theta pinches. We in Garching are also considering toroidal configurations, but no project as yet exists. We believe that there are many problems to be solved first in our linear theta pinches.

Our main interest is devoted to very hot and dense high ß-plasmas, collisionless compression and turbulent heating, and M & S - experiments. The following remarks deal with such questions as preionization, heating processes, end losses, anisotropy and relaxation and instabilities.

The experiments were performed with the capacitor banks Isar I, III and IV (Isar II is not yet finished) and a bank for turbulent heating experiments. Fig. 1 shows that the parameters of the banks are quite different. Isar IV is extremely fast, but the coil is only 14 cm long. Therefore, it is only suitable for studying the initial dynamic behaviour, whereas later on end losses complicate the interpretation. Isar I, with a coil length of 150 cm and a half-cycle of 19 µsec, has a relatively long confinement time. A very hot but anisotropic plasma is produced and the effects of end losses, relaxation and instabilities can be observed. Isar III lies between the two experiments. It is more flexible than Isar I, and so the influence of mirrors on end losses and instabilities was studied.

Preionization

The highest ion energies are obtained in the low pressure regime. The conditions for good preionization, namely a high degree of ionization, high conductivity, low trapped fields and small amounts of impurities, are not easy to fulfill for low initial densities. Three methods are investigated, the high frequency theta pinch, the z-pinch and ultraviolet preionization.

High frequency theta pinch

Apart from the normal theta pinch preionization, we used a method where the frequency of the compressing B-field was in the region of the frequency of the radial plasma oscillations [1] . When the plasma oscillates in phase with the compression field, violent contact with the tube walls occurs and a high degree of impurities is observed. When the frequency is raised, the plasma can no longer follow the magnetic forces and is dynamically confined around the coil axis. Proper controlling of the magnetic field amplitude, frequency and filling pressures higher than 30 /u, results in a well-confined and fairly clean plasma. The streak pictures in Fig. 2 give an impression of the possible phenomena. On the left one can see the effect of pressure variation. For low pressure values the plasma hits the wall. Medium pressure results in a rather stable plasma column well clear of the wall. At higher pressures the plasma is also confined, but assumes a hollow cylindrical shape. On the right one can see quantitatively the same sequence of phenomena, but shifted to higher pressures due to the enhancement of the magnetic field amplitude from 3.9 to 6.3 kG. When the plasma hits the wall an impurity level of about 2 percent oxygen is found, and when the plasma is confined the level drops by an order of magnitude.

A magnetohydrodynamical three fluid model [2] including the neutral gas component is applied to calculate the radial density distri-

bution as a function of time (Fig. 3). The results agree qualitatively with the experimental effects [1] .

Z-pinch preionization

In the low pressure regime, fast theta pinch preionization became unsatisfactory for two reasons. The high voltages required for breakdown could not be applied any more to the theta pinch coil without triggering the main discharge. Furthermore, a fast theta pinch causes high current densities close to the tube walls and thereby releases considerable amounts of impurities. The impurity content of the plasma became a severe problem since the amount of contamination essentially remained the same, whilst the filling pressures were lowered, thus increasing the percentage of impurities. A z-pinch, using a transmission line overcomes the technical difficulties. The current pulses, however, lasted too long (5-10 µsec) and the plasma was considerably contaminated as a consequence of instabilities. A reduction of contamination by an order of magnitude was obtained by a succession of two high voltage z-pinches of short duration [3] . The first one is a two stage 80 kV Marx generator to provide breakdown. Because of its irreproducibility, this discharge is not suited for preionization. A second 120 kV Marx generator follows with a proper delay, compressing and heating the gas in a reproducible and macroscopically stable way. For filling pressures below 5 µ breakdown becomes extremely difficult.

Ultraviolet preionization

All these methods fail at densities below 10^{14} cm^{-3}, which are used in collisionless compression experiments. Here, preionization by strong ultraviolet radiation is applied [4] . The ultraviolet radiation source must fulfill the following conditions: The radiation pulse should be short compared with the recombination time of the ionized deuterium, which is about a few µsec. As much as

possible of the radiation intensity should lie below the limit of ionization of deuterium (800 Å). Theoretical considerations [5] indicate that a deuterium plasma with high density and temperatures above 3 eV yields the most effective radiation. Fig. 4 gives schematically the experimental arrangement. Two fast, high voltage (120 kV) z-pinches on each end of the theta pinch coil are triggered simultaneously. By a pulsed gas inlet, a gas pressure well above the filling pressure for the theta pinch is produced in the z-pinch regions. The degree of ionization in the centre of the coil is 4.5 percent (Fig. 4). The best conditions can be found by properly choosing the delay time between gas inlet and z-pinch ignition. Fig. 5 gives the degree of ionization as a function of this delay time. The ionized plasma consists mainly of D_2^+ ions and a few percent D^+ and D_3^+ ions, as measured with a mass spectrometer [6].

Early phases of a very fast theta pinch (Isar IV)

The above-mentioned double z-pinch preionization is adopted in the Isar I, III and IV experiments. During the first implosion, the magnetic field is measured by probes in Isar IV. The result is shown in Fig. 6. The width of the current layer is fairly large and decreases with increasing pressure (10 μ to 60 μ). The reason for this field diffusion is not yet clear. It is of interest that the magnetic field on the axis remains well below 100 G up to the first compression. Further experiments aim at an improvement of the preionization.

Anisotropy and relaxation

It seems reasonable to assume a highly anisotropic plasma in the Isar I experiments (also in Isar III and IV), and we looked for methods of measuring anisotropy and relaxation effects. The high neutron yield in these experiments allows two different neutron diagnostic methods [7]:

1. Measurement of the neutron energy distribution, for instance with nuclear plates. An example is given in Fig. 7. Here, a) is taken end on parallel to the magnetic field and b) side on, perpendicular to it in the midplane of the coil. The unfolded half-width of the energy spectrum side on is about 18o keV. The end-on spectrum practically coincides with the apparatus profile. This result demonstrates the anisotropy and can be explained by an average perpendicular ion temperature of about 4 keV. Clearly, this value is an average over the time dependent anisotropic ion energy, but the highest energies dominate, as they produce also the highest neutron flux.

2. The anisotropy of the neutron flux [7] . The differential cross section $\sigma(g,\theta)$ for the d (d,n)He^3 reaction is given by the expression:

(1) $$\sigma(g,\theta) = A(g)\left[1 + B(g)\cos^2\theta\right]$$

B(g) is, according to the experimental results of Booth, Preston and Shaw [8] ,

(2) $$B(g) = 0{,}31 + 0{,}0058\,\frac{m}{2}\,g^2$$

$\frac{m}{2}\,g^2$ is the relative energy of the ions in keV. From the anisotropic ion velocity it therefore follows that the neutron flux is anisotropic. It depends on the kind of distribution function. As an example, a two-dimensional Maxwellian may be assumed. Then the ratio of neutron flux perpendicular to the magnetic field $F_\perp$ to the parallel flux $F_\parallel$ as a function of the perpendicular ion temperature $T_{i\perp}$ is:

$F_\perp/F_\parallel$	1,2o	1,24	1,28	1,36
$T_{i\perp}$(keV)	1	3	5	1o

$T_{i\parallel} = 0$ is assumed.

With two scintillators side and end-on, the neutron flux ratio as a function of time was measured. Fig. 8 is a typical example. In these preliminary experiments we were not able to measure the absolute flux ratio and only the variation with time should be regarded. From the experiments it follows that the flux ratio, i.e. the anisotropy, rises rapidly to a maximum well before the field maximum and then falls relatively fast. This slope cannot be explained only by ion-ion collisions. In general, electron-ion collisions and collective interactions must be added. These effects are important for small ratios T_e/T_i. In our experiments T_e reaches about a few 100 eV. The perpendicular ion temperature $T_{i\perp}$ is about 5 keV, calculated from the neutron flux, assuming a prevailing two-dimensional Maxwellian. From theoretical considerations [9] it follows that with $T_e/T_i \approx 10^{-1} - 10^{-2}$ electron-ion collisions are an important factor for relaxation, but not collective interactions. In this case, the problem can be treated with the Fokker-Planck equation. An initially elliptic distribution is assumed to remain approximately elliptic during the relaxation process and the time behaviour of both $T_{i\perp}$ and $T_{i\parallel}$ is calculated for ion-ion and ion-electron collisions for large anisotropy. These results are applied to the Isar I data [10] and the theoretical and experimental values of $T_{i\perp}$ and $T_{i\parallel}$ are compared in Fig.9. $T_{i\perp}$ is taken from the neutron yield, $T_{i\parallel}$ from the end losses, measured by interferometric means.

End losses in mirrorless coils (Isar I)

The end losses are measured with a Mach-Zehnder interferometer. Examples of streak and framing pictures with a Beckmann camera are given in Fig. 10. Fig. 10b is a zero order interferogram. The time behaviour of the total number of particles yields, at least qualitatively, the parallel velocity of particles and consequently the parallel temperature $T_{i\parallel}$. A collisionless

outflow of particles parallel to the magnetic field is assumed.

End losses with mirrors

The relaxation experiments on Isar I are restricted by the short confinement time. Before applying mirrors on Isar I, the influence of mirrors on confinement time and stability was studied in Isar III. Mirror ratios up to R = 3 were applied. The plasma parameters were varied by changing the filling pressure from 10 μ to 40 μ. The ion temperatures lie between 0.5 and 2 keV. It is of interest that for all mirror ratios no instabilities could be seen in streak camera pictures during the observation time of about 5 μsec. This is demonstrated in Fig. 11, where streak pictures are taken along the coil axis, including also the mirror regions. No indication of instabilities can be found either in the time behaviour of the end losses. It must be mentioned that rotational instabilities occasionally arise with and without mirrors. Also in a very short mirror, instabilities are indicated by an abnormally high loss rate. These effects are not yet fully understood.

As in Isar I, the loss rate can be described by collisionless outflow along the field lines. In contrast, however, to Isar I, the experimental values of Isar III agree with this model, on the assumption that $T_{i\parallel} = T_{i\perp}$. This means that $v_{\parallel}$ equals the thermal velocity v_{th}. Such an assumption seems reasonable considering the influence of mirrors. In this experiment, the mirror regions dominate since the coil length is short. Axial compression in the initial phases produces particles with parallel velocities and increases the density as well. Furthermore, the ion temperature is lower than in Isar I. Therefore, the anisotropy is reduced.

It follows from these experiments that the confinement time t_N rises about proportionally to the mirror ratio R:

$$t_N \sim \frac{R}{v_{th}} \sim \frac{R}{\sqrt{T_i}}$$

With R = 3, for instance, $t_N \approx 7{,}5\,\mu$sec is measured, instead of $t_N \approx 2\,\mu$sec for R = 1.

In Fig. 12 t_N is plotted as a function of R for different initial pressures. The measured values are compared with calculated values from the collisionless outflow model [11] and from the magnetohydrodynamic model of Taylor and Wesson [12]. These results seem encouraging enough to continue the Isar I relaxation studies with mirror coils.

Ion and electron temperatures and densities from laser scattering experiments

Electron temperatures on Isar I were measured by 90° laser scattering. The values are plotted as a function of the bank voltage in Fig. 13. T_e values as obtained from soft X-ray absorption are compared with the laser data and show quite irregular behaviour. The time of observation after the ignition of the theta pinch is also given in the figure. It seems that X-ray absorption is not well suited in our fast compression experiments at low densities. The reasons could be deviations from a Maxwell distribution of the electrons or impurity radiation.

Ion temperatures on Isar III were obtained from forward laser scattering [13]. In another experiment [14] we fulfilled the condition for cooperative scattering $\alpha = 1/kD \gg 1$ by reducing the Debye length D, whereas the scattering angle was 90°. This means a plasma of high density, a few 10^{17} cm^{-3}, and low temperature, a few eV. The spectrum of the ion line

was measured as well as the position and half-width of the satellite lines. The spectrum was obtained from a single discharge with an error of ± 5 percent. Fig. 14 and Fig. 15 show examples.

Theoretical curves according to the Salpeter theory are properly fitted to the experimental values. The theory now yields the parameter β , a function of α and the ratio T_e/T_i. The shape, the half-width, the total intensity of the ion and satellite lines and the frequency distance between the centres of the ion and satellite lines make it possible to evaluate the ion and electron temperature and density. The electron density can be found by three independent methods: a) from the shape of the ion line, b) from the distance ion - satellite line and c) from the ratio of total intensity of the ion line to the satellite line. All methods agree within the limits of experimental errors.

The half-width of the satellite lines greatly exceeds the values predicted by the collisionless scattering theory. Nor can the difference be explained by the influence of collisions. On the other hand an electron density variation of about 1o percent in the scattering volume leads one to expect the measured half-width.

The theory assumes a number of electrons in the Debye sphere $nD^3 \gg 1$. With the proper choice of plasma parameters in these experiments nD^3 varies between 2 and 1o. Even for $nD^3 = 2$, good agreement within ± 5 percent between theory and experiment is found. The theory holds also for a few electrons in the Debye sphere.

Two-dimensional programmes

A two-dimensional programme with rotational symmetry (r,z) has been developed for the computation of end losses in theta pinches with and without mirrors [15] . It has reached its first stage, in which a relatively simple plasma model is used. It is

a one fluid model with isotropic pressure and infinite electrical conductivity. Furthermore radial equilibrium for all times is assumed. The influence of thermal conductivity is taken into account, however.

It appears interesting to compare the results for zero thermal conductivity with those for nonzero conductivity. For a special case (Isar III, B_m = 7o kG, n = 6 · $1o^{16}$ cm^{-3}, T = 4oo eV, coil length = 3o cm), the confinement times with and without thermal conductivity are 1.7 /usec and 1.3 /usec respectively. It is a general feature that thermal conductivity increases the confinement time as a consequence of the reduced temperature. In Fig. 16, Fig. 17 and Fig. 18 density, temperature and pressure along the axis are shown as a function of time. With conductivity, the density increases even initially and falls slowly as compared with the case of zero conductivity. The temperature, on the other hand, falls to lower values with conductivity. The pressure shows similar behaviour. Fig. 19 presents the energy losses as a function of time with and without conductivity. With conductivity the rate of energy losses is larger in the early phases of the pinch. The results agree qualitatively with the experimental values in Isar III with a mirrorless coil. This comparison is preliminary, however, and a final comparison will be made once a two fluid model with anisotropic pressure has been included in the programme.

A two-dimensional (r, φ) programme has also been developed [16] . A fairly complete set of two fluid equations, including thermal conductivity, Hall term, exchange of energy between ions and electrons, finite electrical conductivity etc. is used. The programme has been applied to the problem of plasma rotation induced by super-imposed magnetic fields perpendicular to the axis. The computations concern the first implosion in Isar III for different filling pressures and trapped fields from -1 kG to +1 kG and perpendicular fields from o.1 - 1 kG. The result is that the plasma does not rotate like a rigid body. The rotational velocity changes

its sign as a function of radius at least once. An example is given in Fig. 2o. Here $n \cdot v_\varphi$ is plotted as a function of r and φ. The rotational velocity develops in about $1o^{-7}$ sec and reaches values of the order of $1o^6$ cm/sec. A second example is given in Fig. 21. Here, a quadrupole field is superimposed. The figure shows the distortion of the magnetic field lines by the plasma rotation.

Collisionless compression and turbulent heating

In fast theta pinches at low densities the collisionless processes are important. In order to evaluate the influence of a two stream instability on the structure of a strong, nonstationary compression pulse, a numerical programme was treated [17]. It uses a two fluid model for a cylindrical plasma including effects of electron inertia and describes the action of the instability by a phenomenological friction term. This friction term limits the azimuthal electron speed to a critical value which, in turn, is connected with the electron temperature and changes, therefore, with heating by friction and compression.

This friction term may or may not prevent density profiles, radial velocity and pressure from running into a discontinuity. This is demonstrated in the density profile of Fig. 22. The density n/n_o is plotted over the radius r/R_o at different dimensionless times τ. At $\tau = 2.4$, the density profile exhibits a sharp peak. Here, fluid elements coming from behind the wave with higher velocities tend to overturn the preceeding ones.

These theoretical predictions are being investigated in a fast theta pinch at low densities between $1o^{12}$ - $1o^{14}$ cm^{-3}. The lowest densities ($1o^{12}$ - $1o^{13}$ cm^{-3}) can be reached only by using ultraviolet preionization, which also has the advantage of producing a radial homogeneous plasma of well-known density. We intend to measure the r and φ components of the electron density by a $9o^o$ laser scattering experiment. An electrostatic particle energy analyzer is being used to measure the energy distribution

of ions and electrons escaping from the ends.

The "Limpus" experiment

As mentioned at the beginning, we shall also have to study toroidal pinches in the future. One possibility is offered by the M & S principle [18] . A preliminary experiment with a linear, corrugated coil (Limpus) has been performed on Isar I [19] . As in a straight coil, instabilities could be observed in the Limpus experiment at $2o/u$, but not at $1o/u$. This is demonstrated in Fig. 23. Further experiments with higher corrugation amplitudes are planned.

References

[1] G.Decker, D.Düchs and H.Herold,
Dynamics of a Plasma in a High Frequency Theta Pinch Discharge
Paper presented at the 1st European Conf.on Plasma Phys. and Contr.Nucl.Fus.Res., Munich (1966)

[2] D.Düchs,
Three-Fluid Model for a Partially Ionized Plasma in Theta Pinch Discharges
Comptes Rendus de la VIe Conf.Intern.sur les Phen.d'Ion.Dans les Gas, Vol.II, 567, Paris (1963)

[3] U.Schumacher and R.Wilhelm,
Ein schneller 12o kV Z-Pinch zur Vorionisierung bei geringen Ausgangsdichten
Paper presented at Tagg.d.Deutsch.Phys.Gesell., Kiel (1966)

[4] G.Hofmann,
Eine Strahlungsquelle hoher Leistung unter 8oo Å zur Photoionisation von Wasserstoff als Vorionisation eines Theta Pinchs
J.Quant,Spectr. and Rad. Transf., in press (1967)

[5] G.Hofmann,
Die Emission dichter Helium- und Wasserstoffplasmen und ihre Brauchbarkeit zur Photoionisation von molekularem Wasserstoff
J.Quant.Spectr. and Rad. Transf., in press (1967)

[6] H.Niedermeyer,
Ein elektrostatischer Analysator zur Messung der Energie von Ionen und Elektronen aus heissen Plasmen
Institut f. Plasmaphysik, Garching, Report IPP 1/66 (1967)

[7] G.Lehner and F.Pohl,
Neutrons and d-d reactions as a tool for plasma diagnostics
Institut f. Plasmaphysik, Garching, Report IPP 1/6o (1967), to be published Zeitschr. f. Physik

[8] D.L.Booth, G.Preston and P.F.D.Shaw,
The Cross Section and Angular Distributions of the d-d Reactions between 4o and 9o keV
Proc.Phys.Soc.69A, 265 (1956)

[9] G.Lehner,
On the Relaxation of Anisotropic Plasmas
Zeitschr. f.Physik, in press (1967)

[1o] C.Andelfinger, E.Fünfer, G.Lehner, H.Paretzke, F.Pohl, U.Seidel, J.Sommer, M.Ulrich
Anisotropy and its Relaxation in a fast Megajoule Theta Pinch
Institut f. Plasmaphysik, Garching, Report IPP 1/67, in press

[11] E.Unsöld,
Die Auswirkung starker magnetischer Spiegel auf das Plasma in einem Theta-Pinch
Diplomarbeit Technische Hochschule München (1967)

[12] J.B.Taylor and J.A.Wesson,
End losses from a Theta Pinch
Nucl.Fus.,5,159 (1965)

[13] B.Kronast, H.Röhr, E.Glock, H.Zwicker, E.Fünfer,
Measurements of the Ion and Electron Temperature in a Theta-Pinch Plasma by Forward Scattering
Phys.Rev.Let. 16, 1082 (1966)

[14] H.Röhr,
Ein 90° Laser Streuexperiment zur Messung von Temperatur und Dichte der Ionen und Elektronen eines kalten, dichten Theta-Pinch Plasmas
Institut f. Plasmaphysik, Garching, Report IPP 1/58 (1967)

[15] F.Hertweck and W.Schneider,
A Two-Dimensional Computer-Programme for Endlosses from a Theta-Pinch
Paper presented at 2nd European Conf.on Contr.Nucl.Fus.Res., Stockholm (1967)

[16] D.Düchs,
to be published

[17] R.Chodura,P.Igenbergs,
Numerical and Experimental Investigations on Collision-free compression of a Plasma with Anomalous Friction
Paper pres. at 1st Europ.Conf.on Contr.Nucl.Fus.Res., Munich (1966)

[18] F.Meyer and H.U.Schmidt,
Torusartige Plasmakonfiguration ohne Gesamtstrom durch ihren Querschnitt im Gleichgewicht mit einem Magnetfeld
Zeitschr. f. Naturf. 13a, 1005 (1958)

[19] C.Andelfinger, G.Decker, E.Fünfer, H.Hermansdorfer, M.Keilhacker, E.Remy, M.Ulrich, H.Wobig, G.H.Wolf,
Preliminary Investigation of a Currugated Theta Pinch ("Limpus") at Isar I,
Institut f. Plasmaphysik, Garching, Report IPP 1/55 (1966)

Fig. 1 Linear Thetapinch Experiments at Garching
(Maximum Operating Values)

Exper.	W kJ	U_o kV	B kG	$\dot{B}$ G/sec	E_φ kV/cm	L_a nHy	Coil l(cm)	Coil d(cm)	T/2 µsec	T_c /e µsec
Isar I	2670	40	170	$2.6 \cdot 10^{10}$	0.7	5.1	150	10	20	105
Isar II	500	2x40	90	$5.6 \cdot 10^{10}$	1.4	8	100	10	5.2	≈50
Isar III	80	40	80	$4.4 \cdot 10^{10}$	0.77	20	30	7	5.8	30
Isar IV	115	2x40	170	$1.6 \cdot 10^{11}$	2.8	7.5	14	7	3.4	50
Turb. Heat. Exper.	9.6	2x40	12	$3.1 \cdot 10^{10}$	1.2	2x6	60	15.8	1.2	8

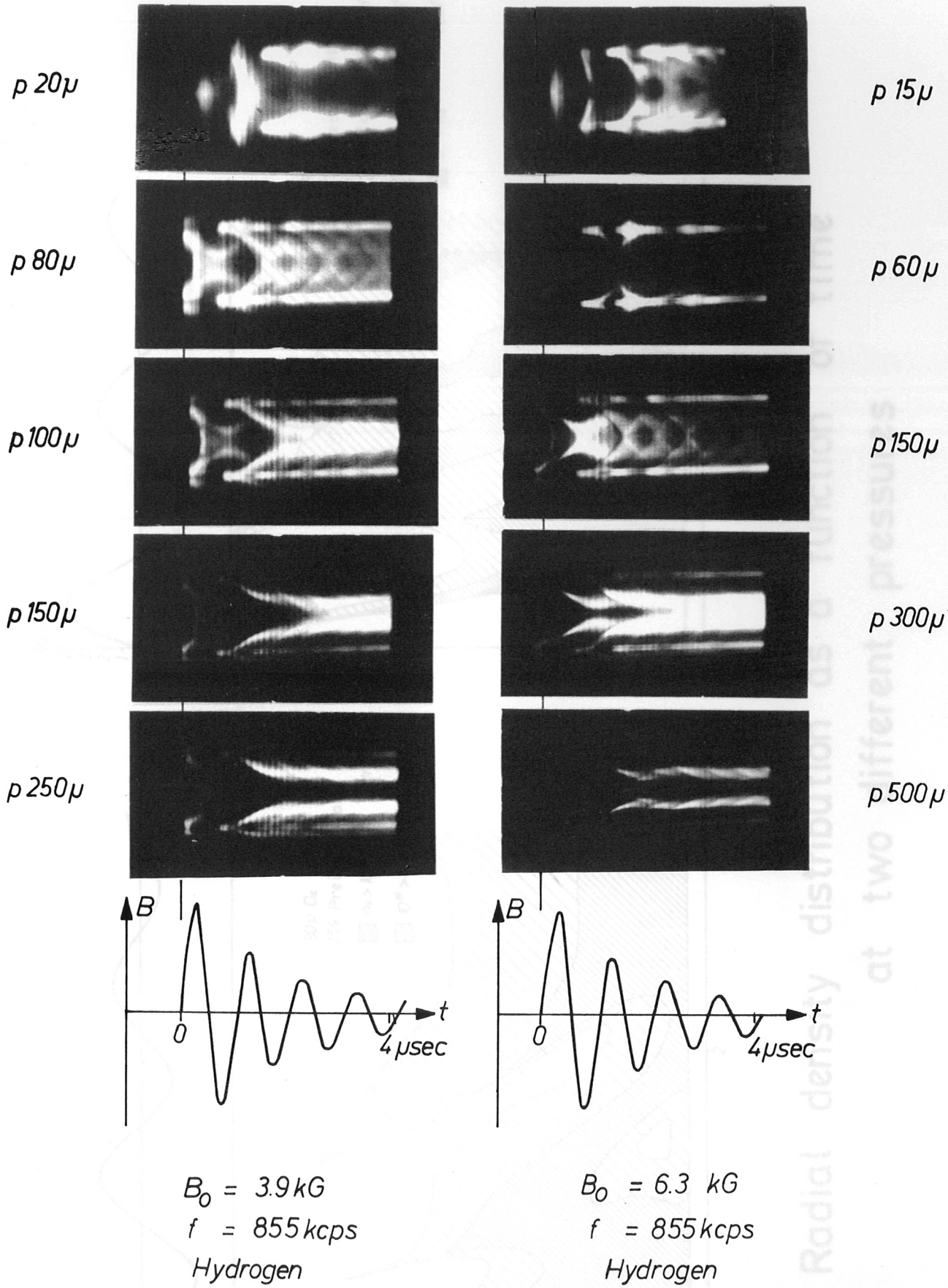

Fig. 2 Streak camera pictures of a high frequency thetapinch at various pressures and magnetic fields

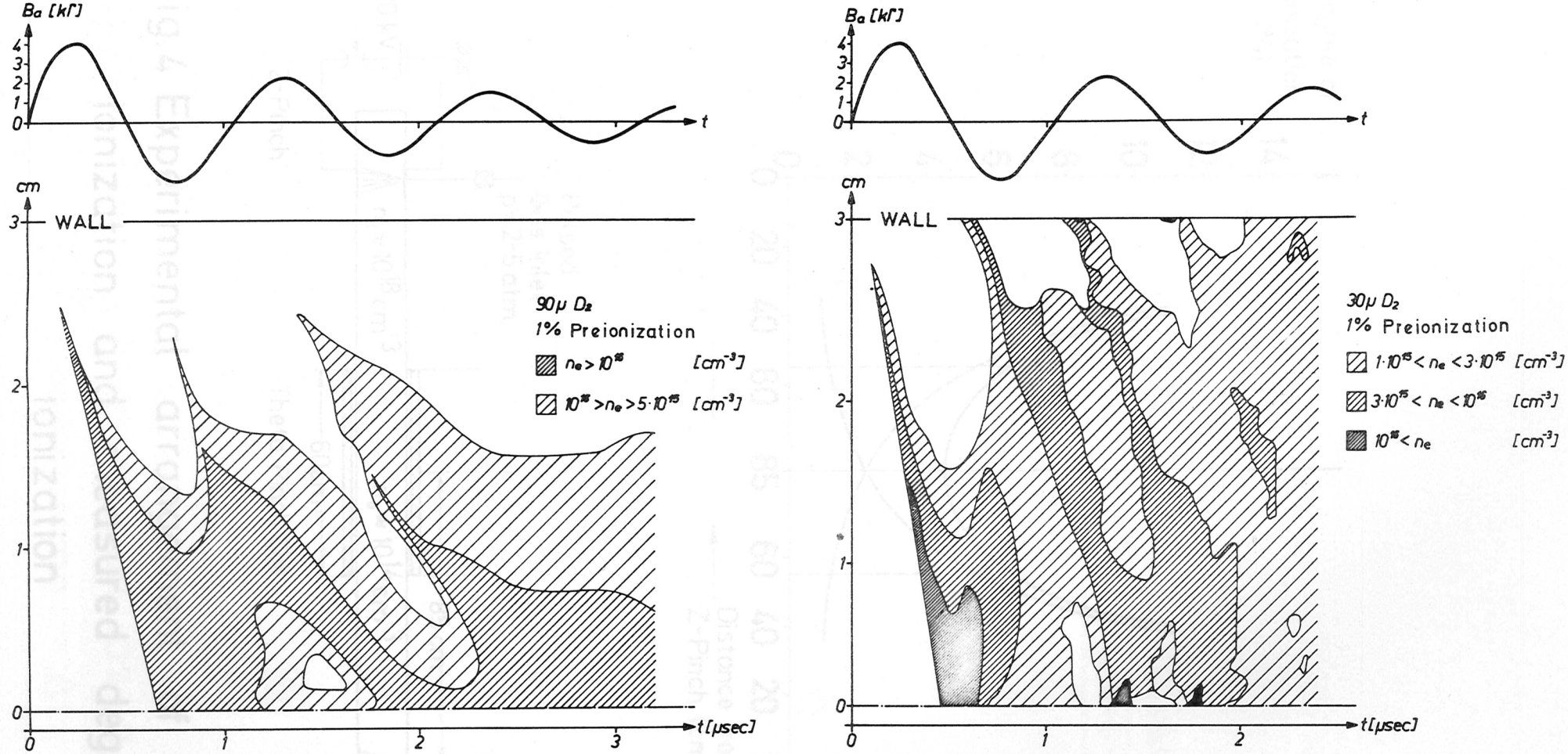

Fig.3 Radial density distribution as a function of time at two different pressures

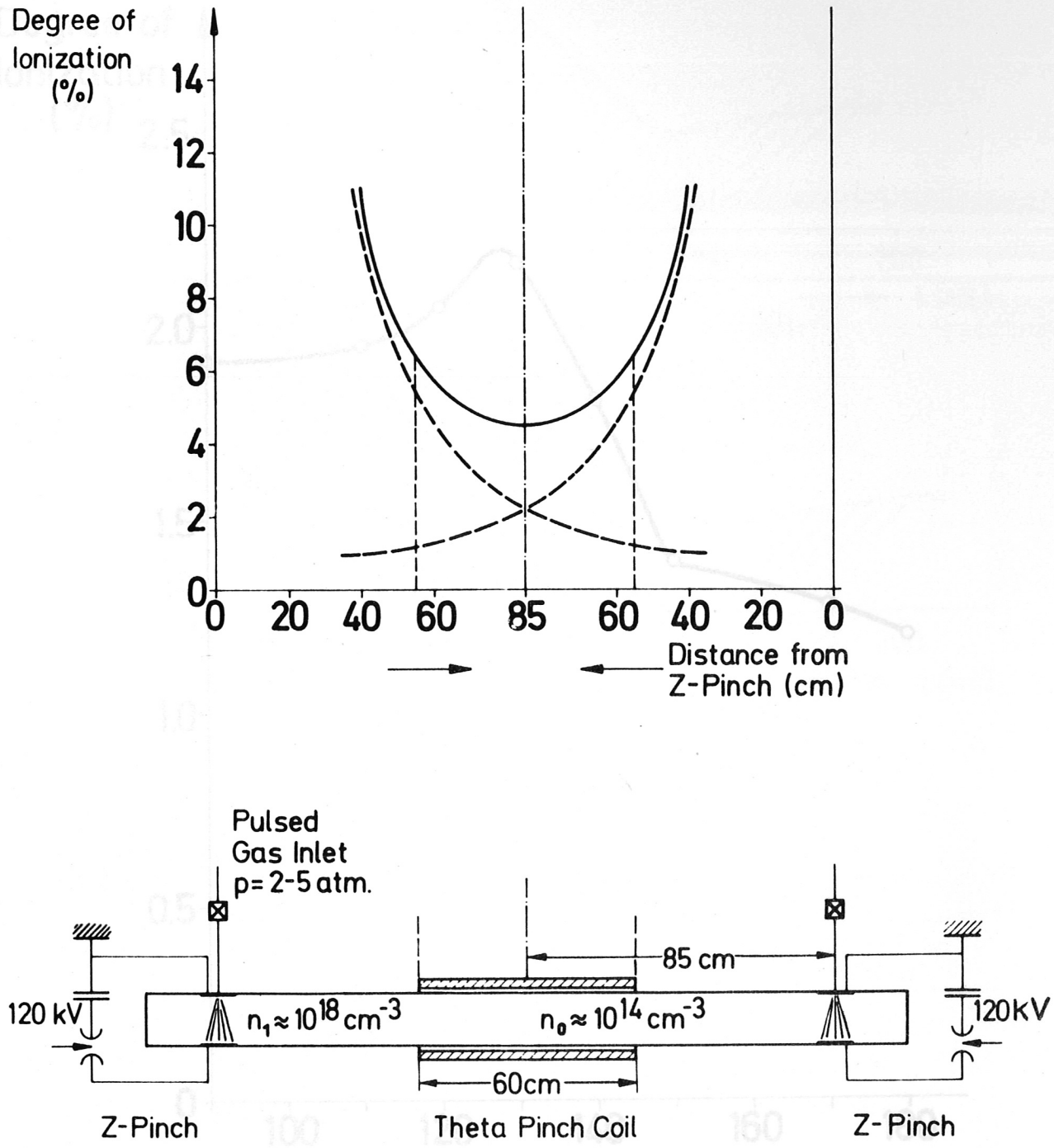

Fig. 4 Experimental arrangement of UV-pre ionization and measured degree of ionization

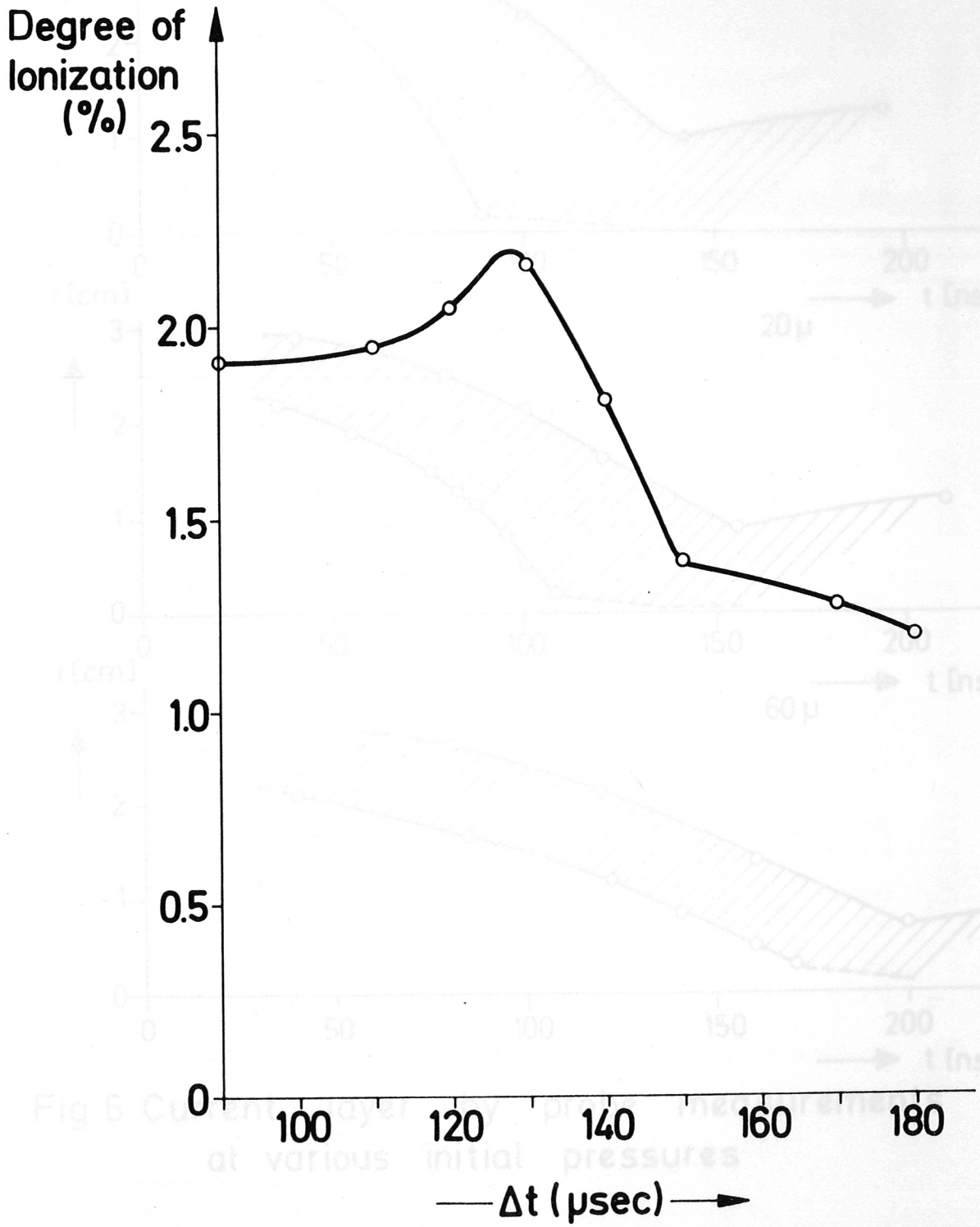

Fig.5 Degree of ionization as a function of delay time Δt

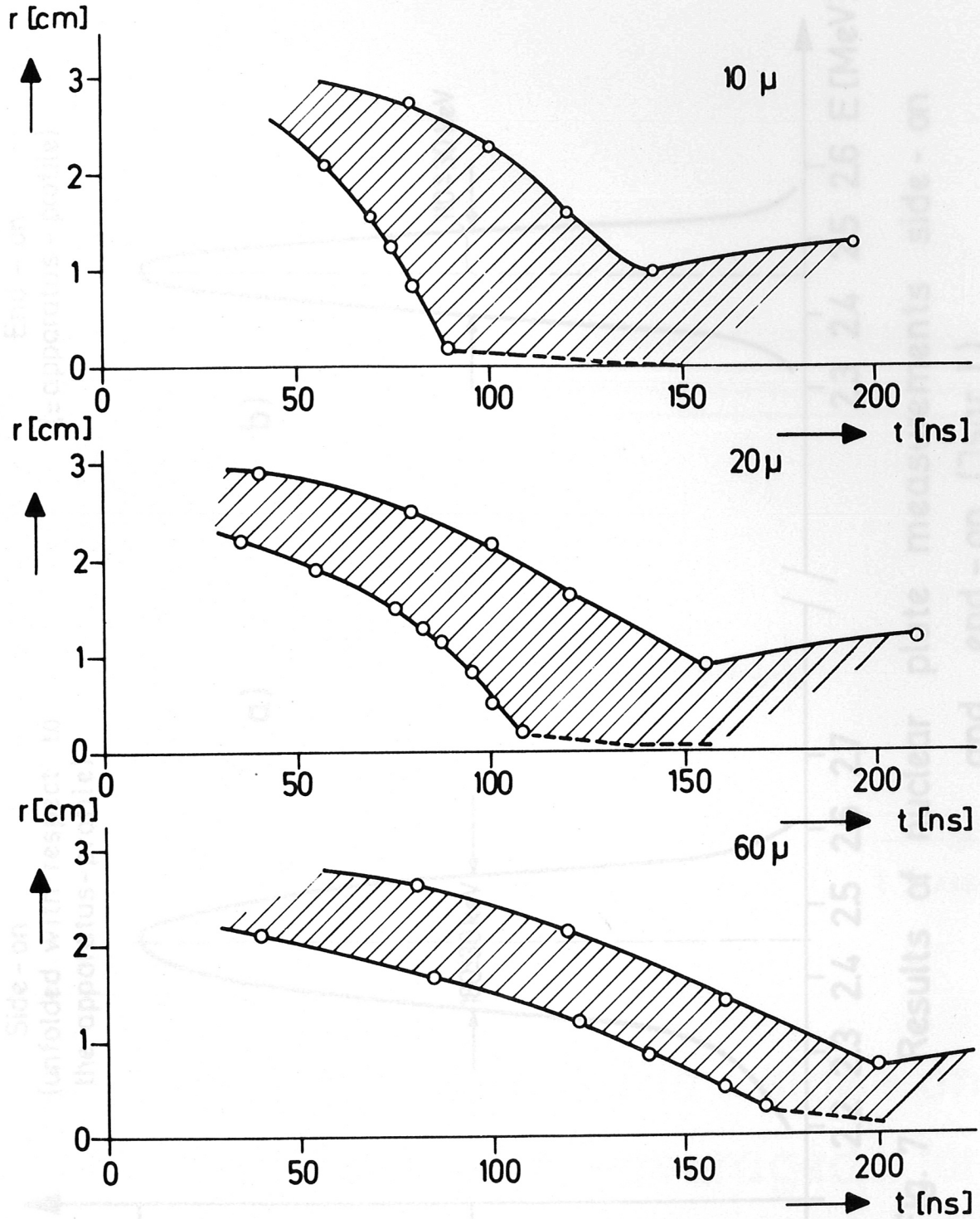

Fig. 6 Current layer by probe measurements at various initial pressures

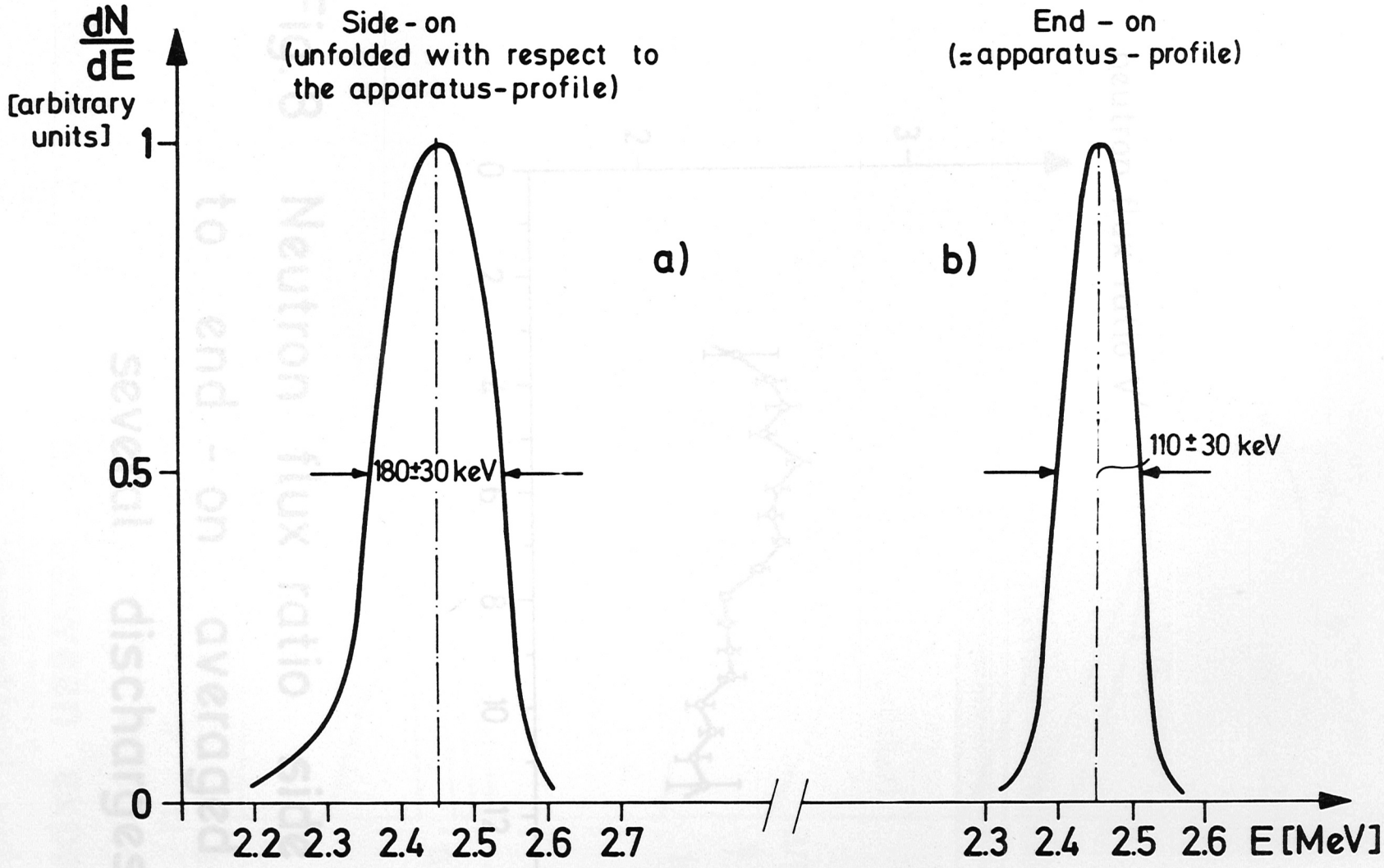

Fig. 7 Results of nuclear plate measurements side - on and end - on (Jsar I)

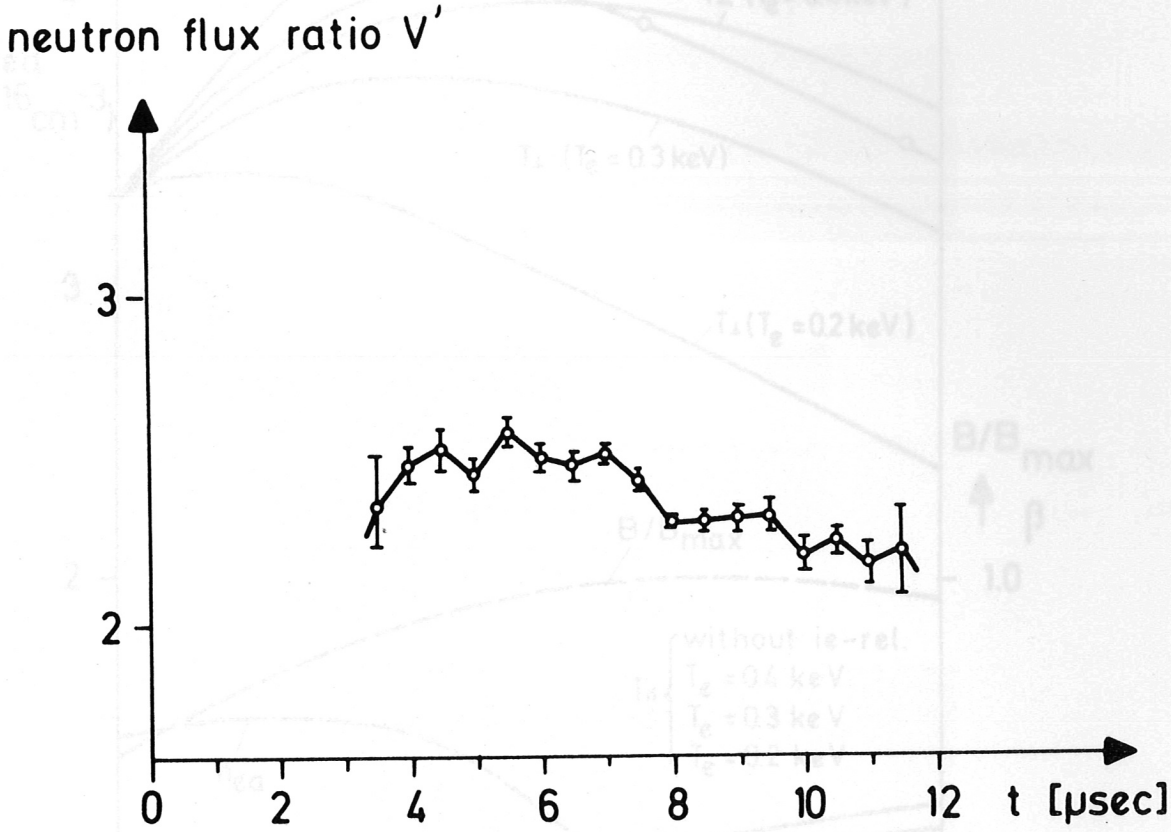

Fig. 8 Neutron flux ratio side - on to end - on averaged for several discharges

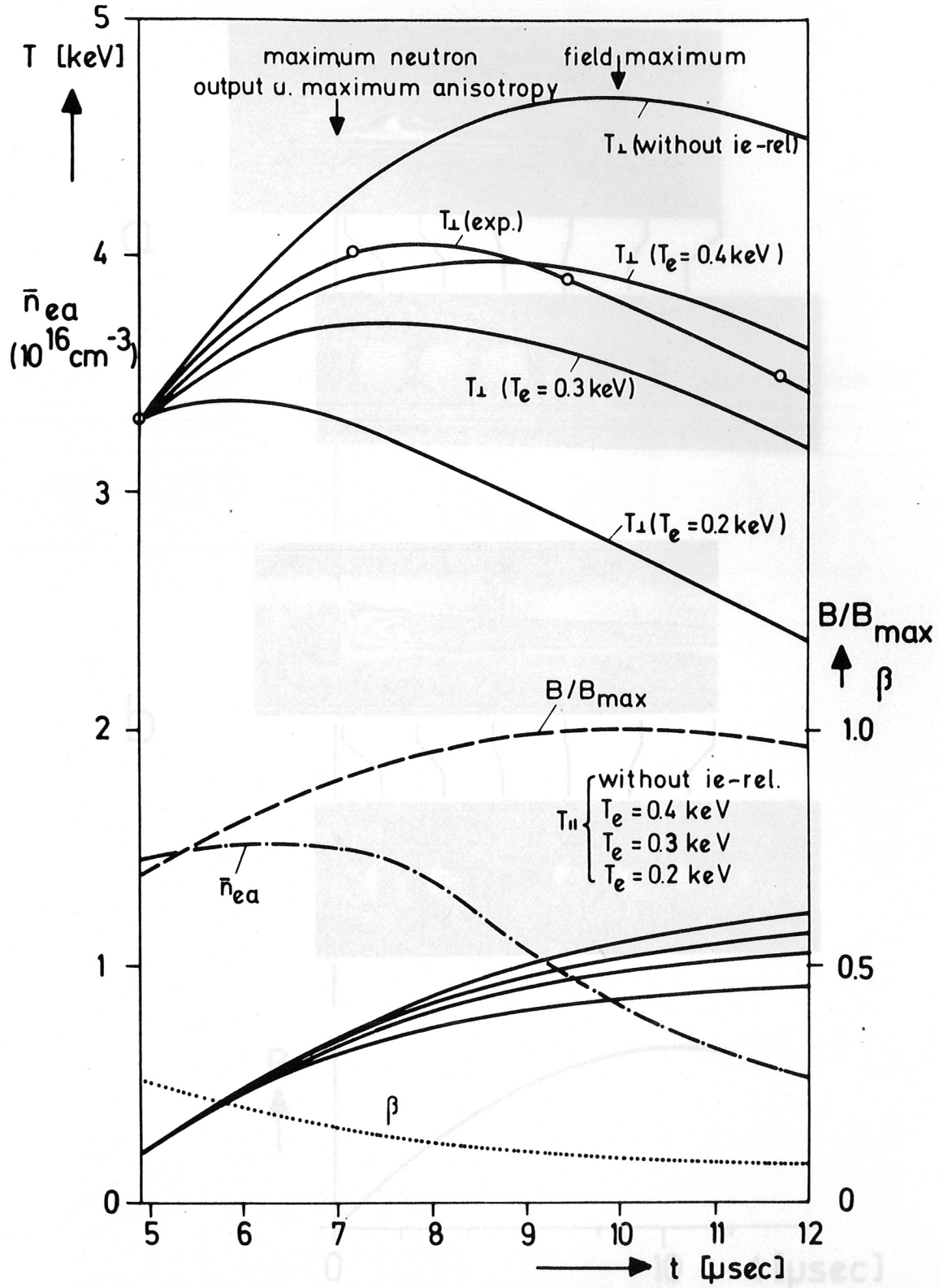

Fig. 9 Comparison between experimental and theoretical values of the temperatures concerning experiments on Jsar I

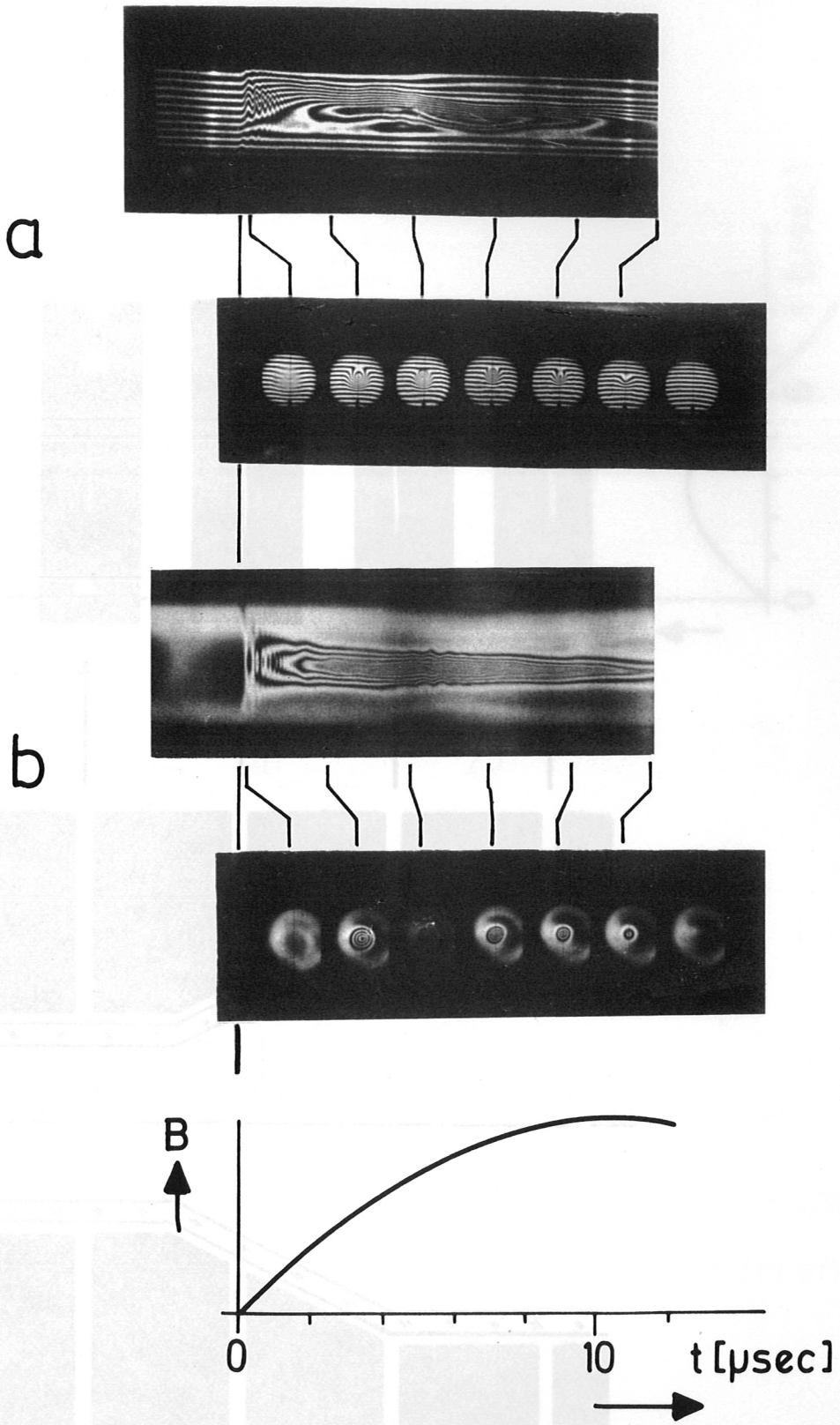

Fig. 10 Streak and framing interferograms

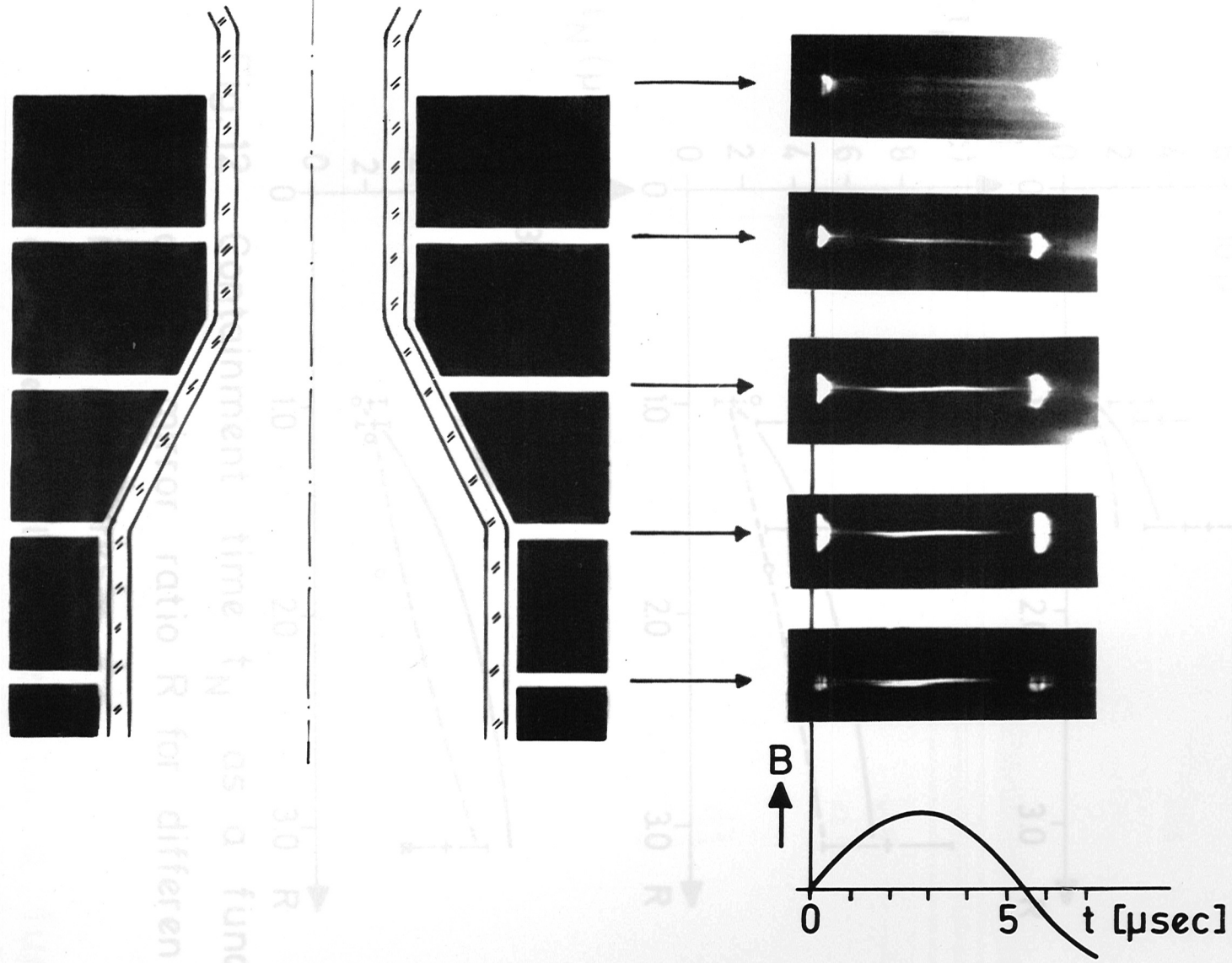

Fig. 11 Streak pictures at various points of the coil axis

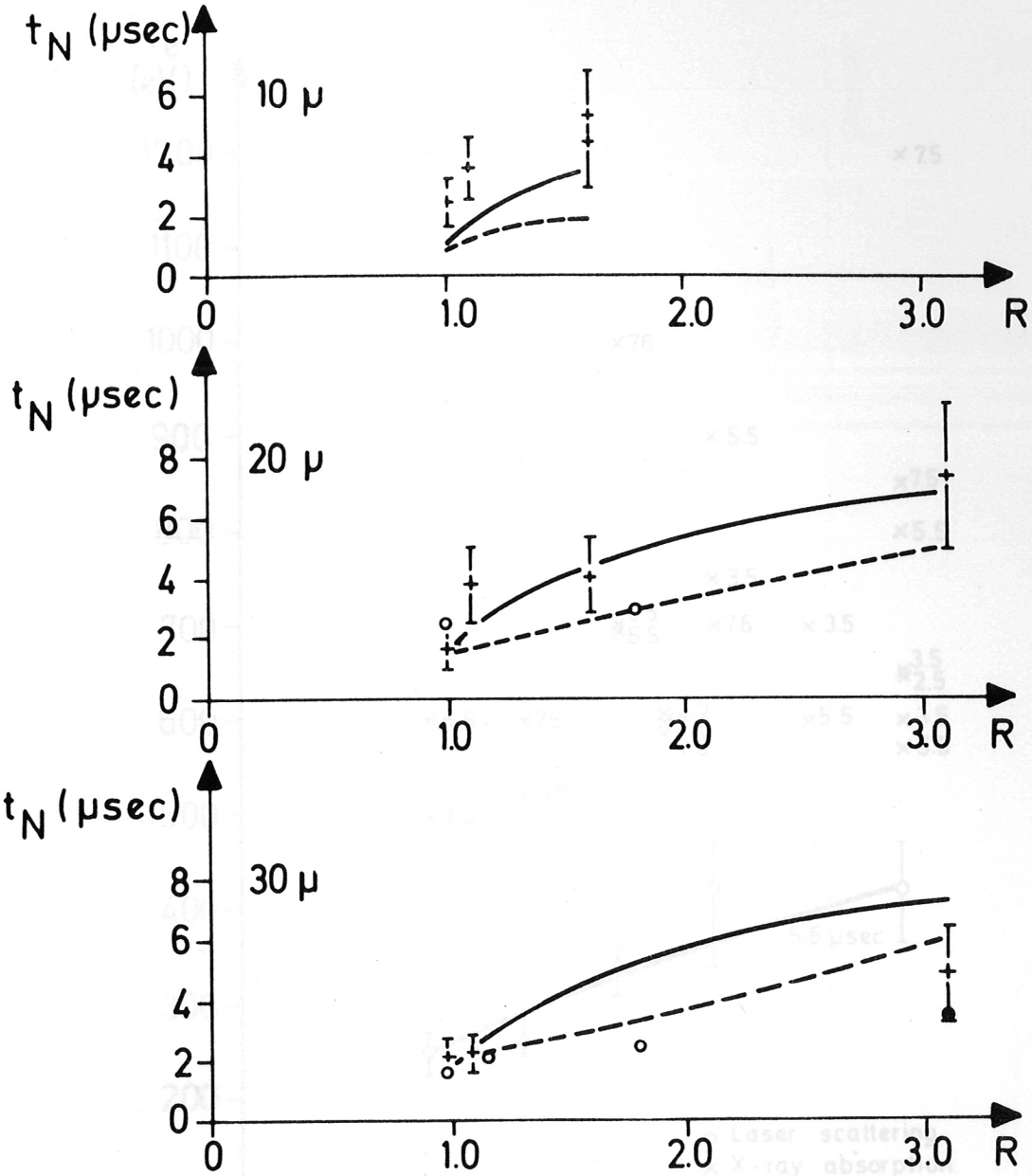

Fig. 12 Containment time t_N as a function of the mirror ratio R for different initial pressures

\+ experimental values

— magnetohydrodynamic model

--- collisionsless outflow model

o twodimensional one-fluid calculations

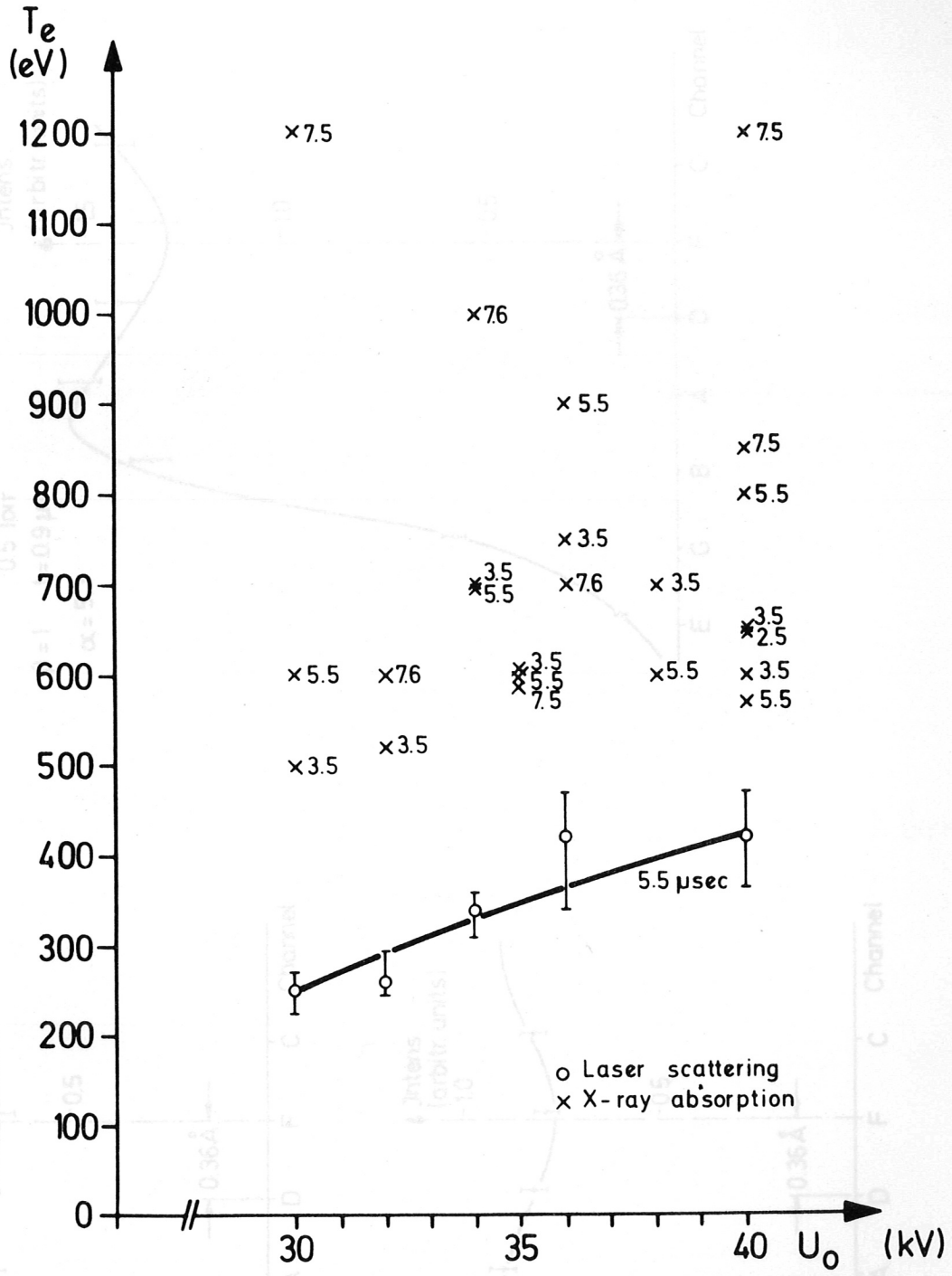

Fig. 13 Electron temperatures as a function of the bank voltage U_o

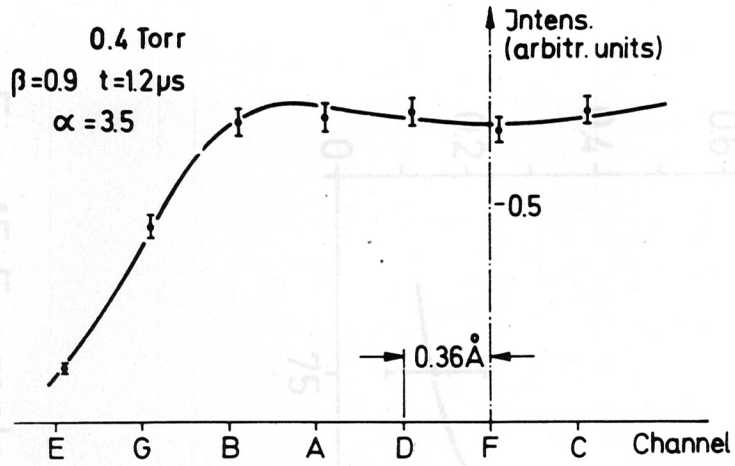

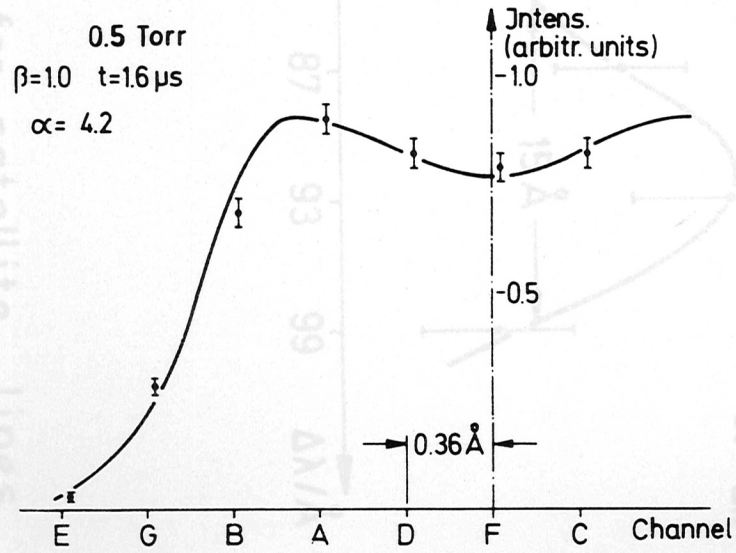

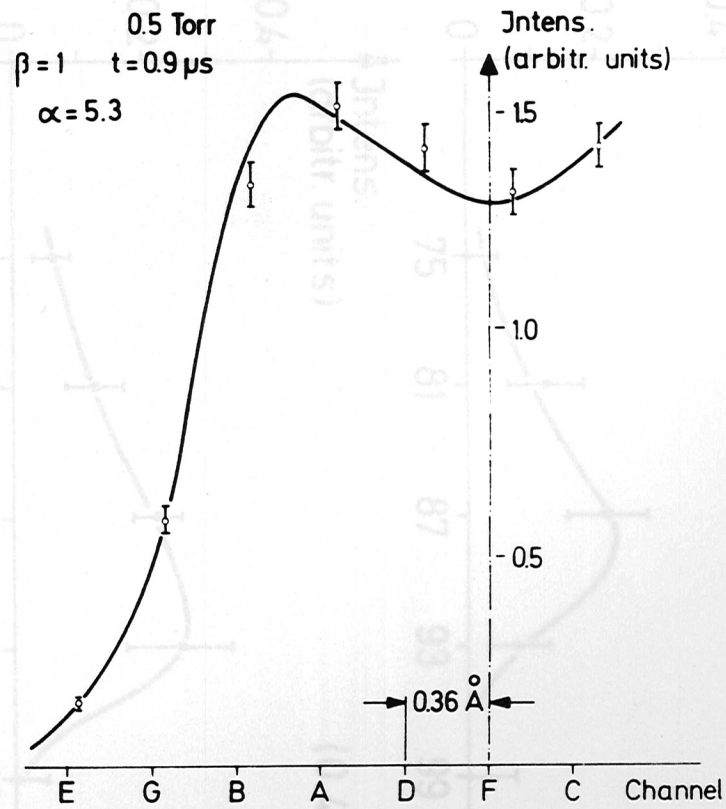

Fig. 14 Spectra of ion lines at various plasma parameters

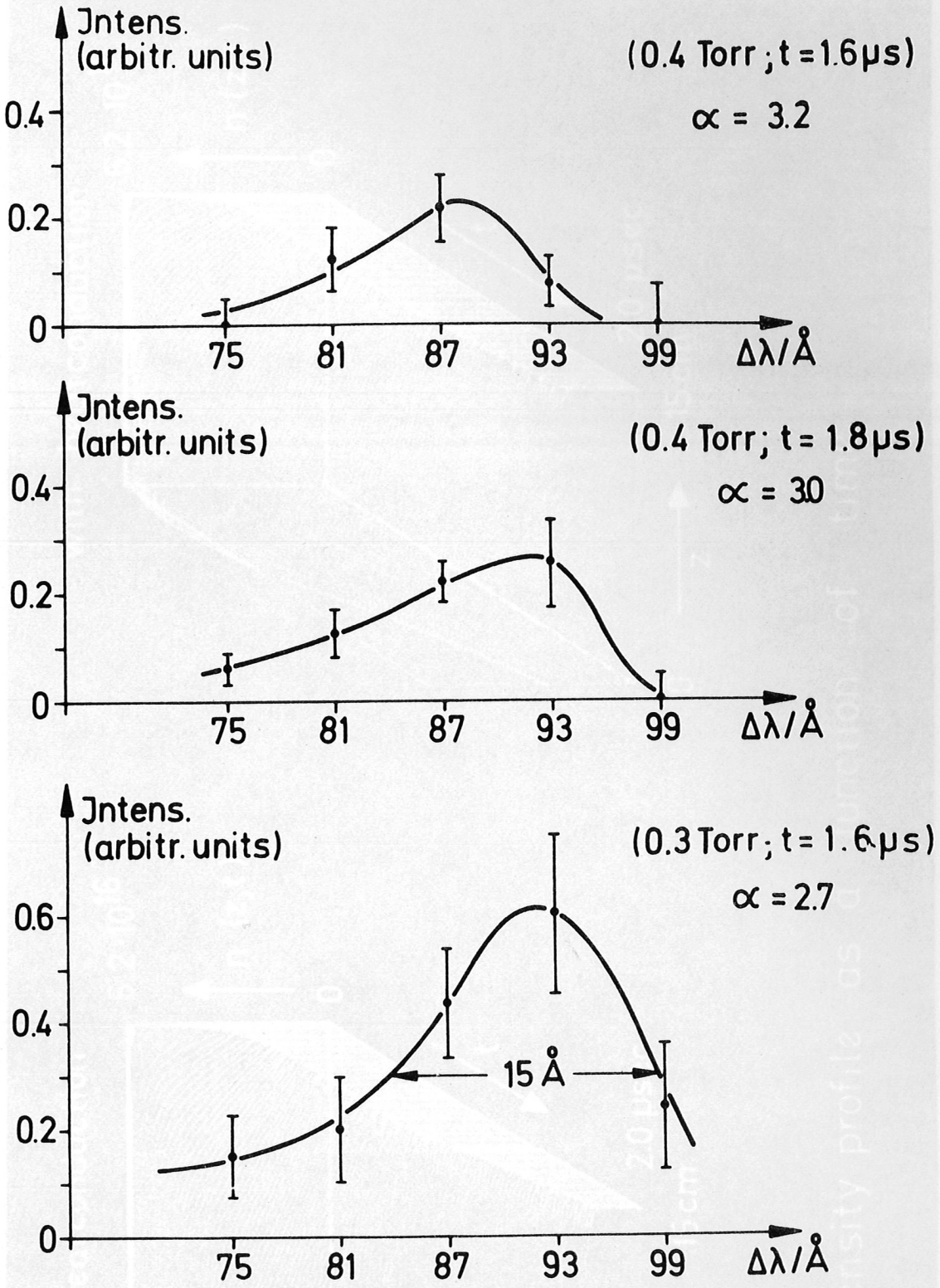

Fig. 15 Examples for satellite lines

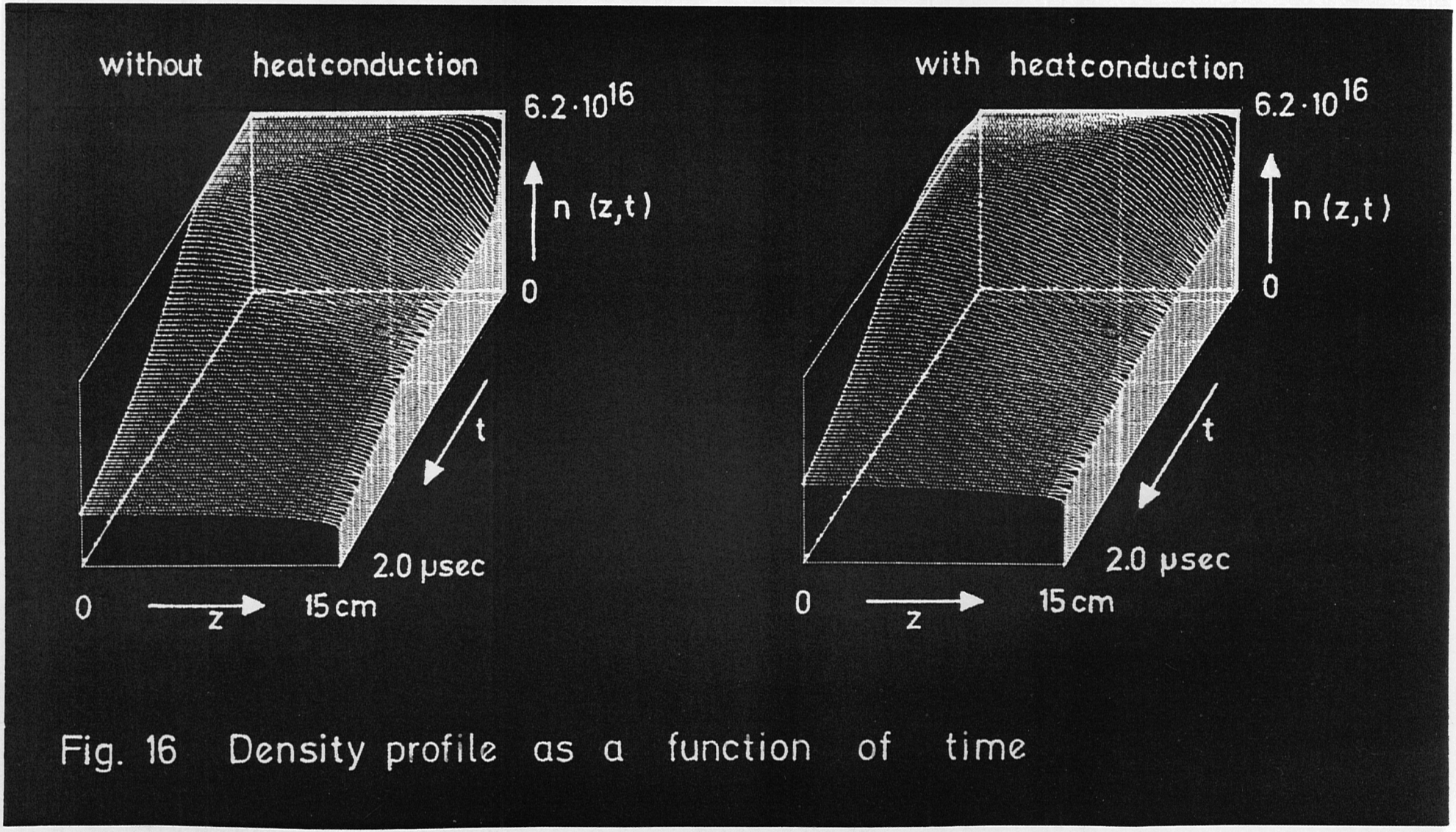

Fig. 16 Density profile as a function of time

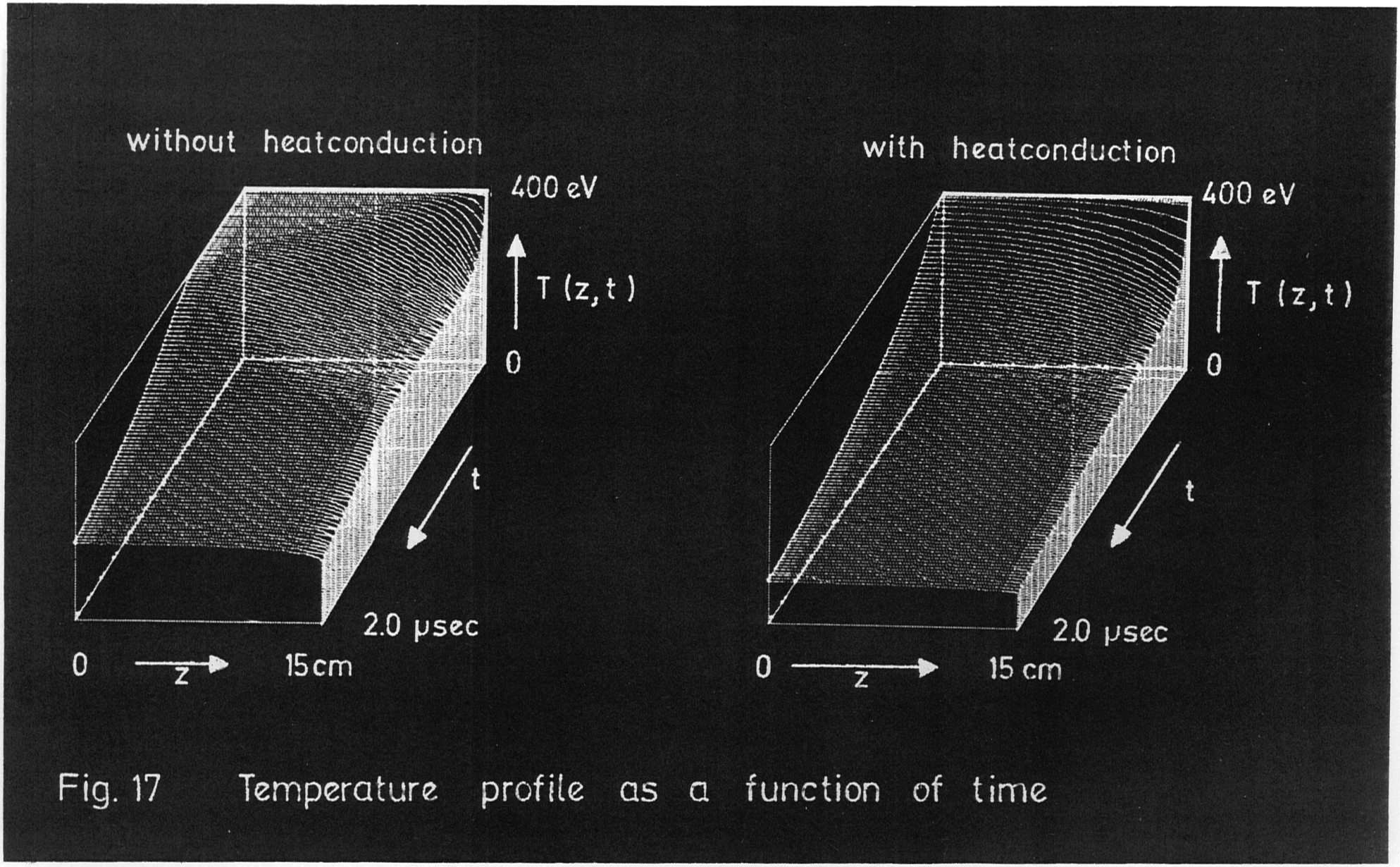

Fig. 17 Temperature profile as a function of time

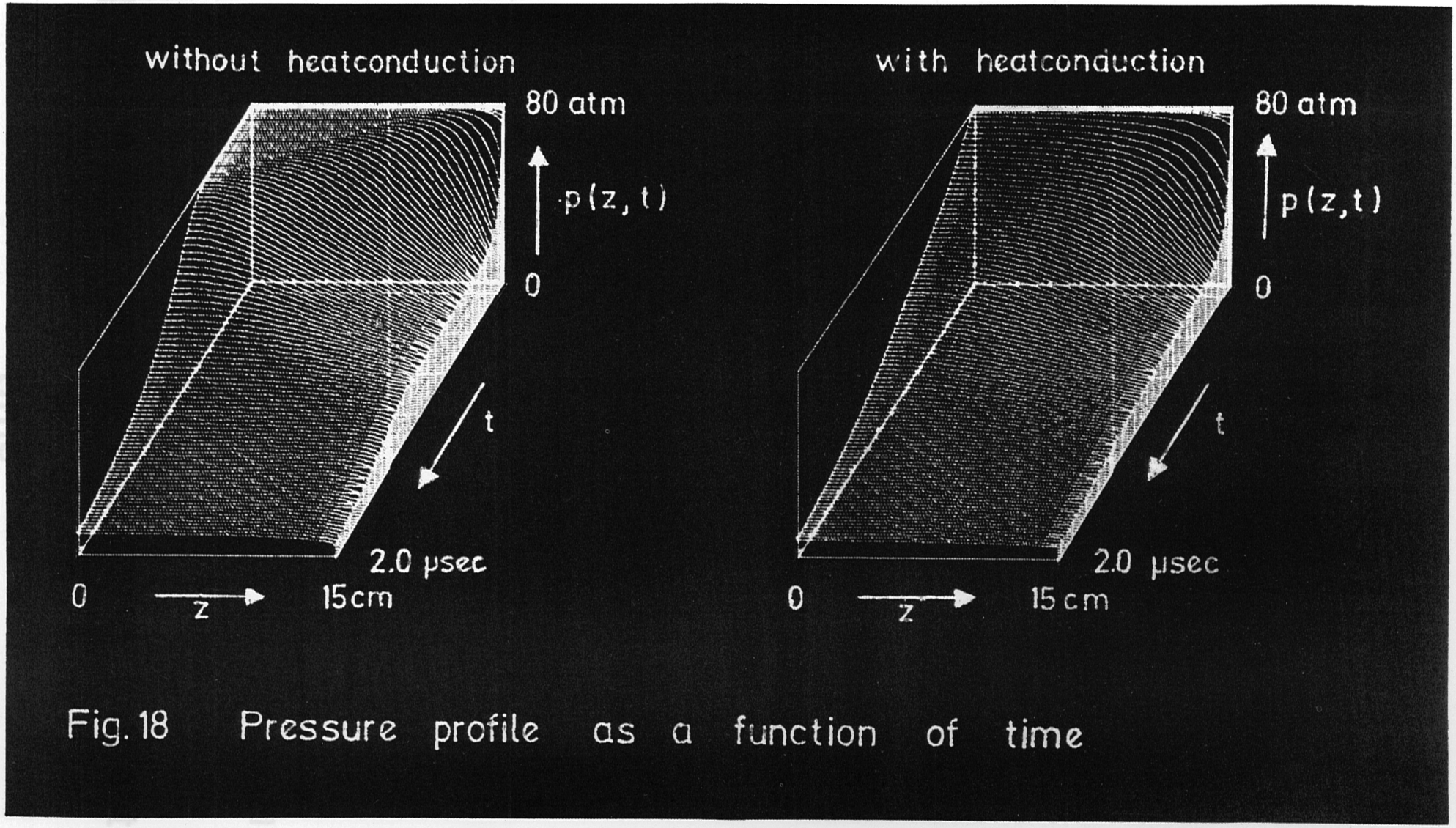

Fig. 18 Pressure profile as a function of time

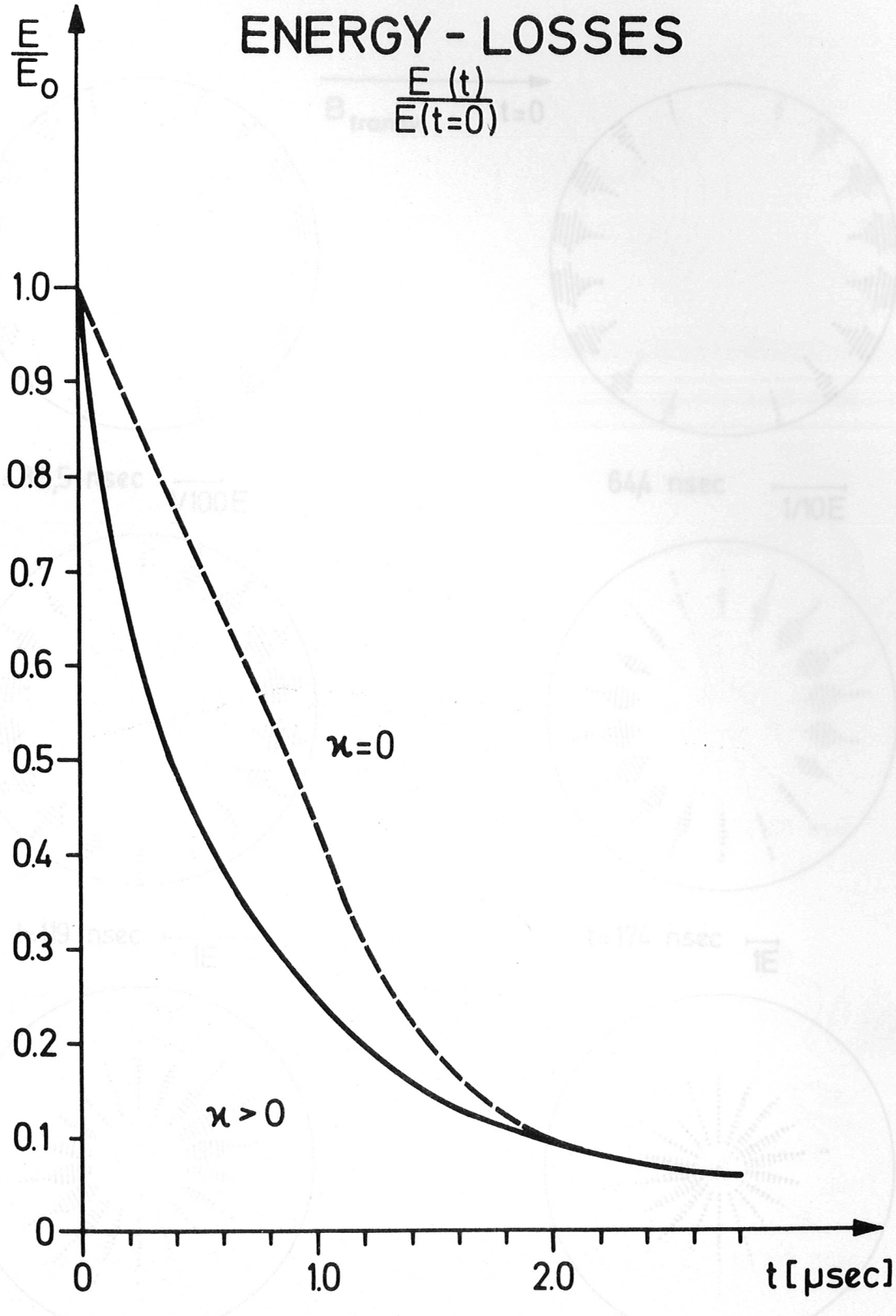

Fig. 19 Energy losses with and without conductivity $\varkappa$ as a function of time

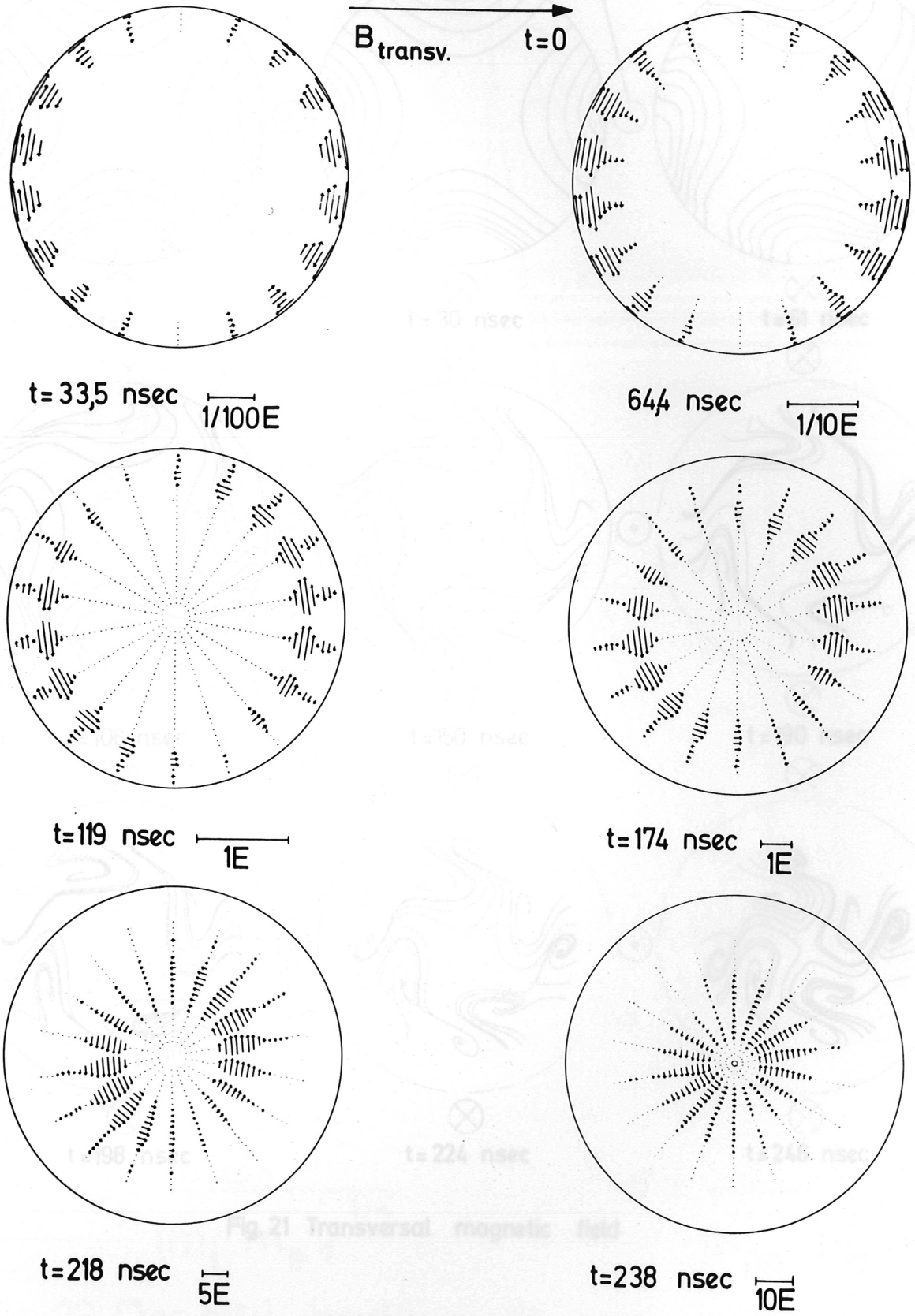

$n \cdot \sigma_\varphi$: 1E = 10^{10} cm sec^{-1} cm^{-3}

Fig. 20 $n \cdot \sigma_\varphi$ as a function of radius, angle and time

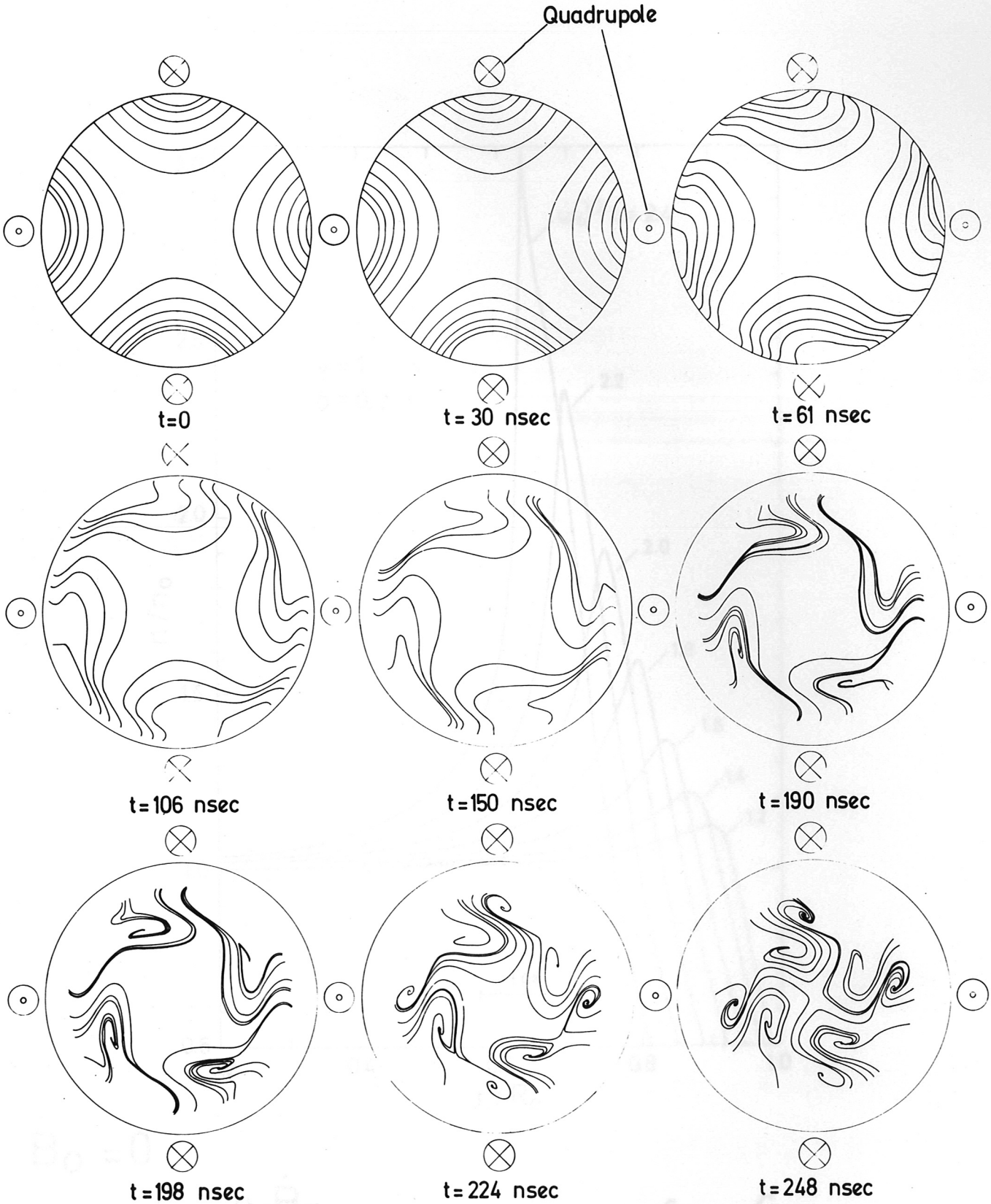

Fig. 21 Transversal magnetic field

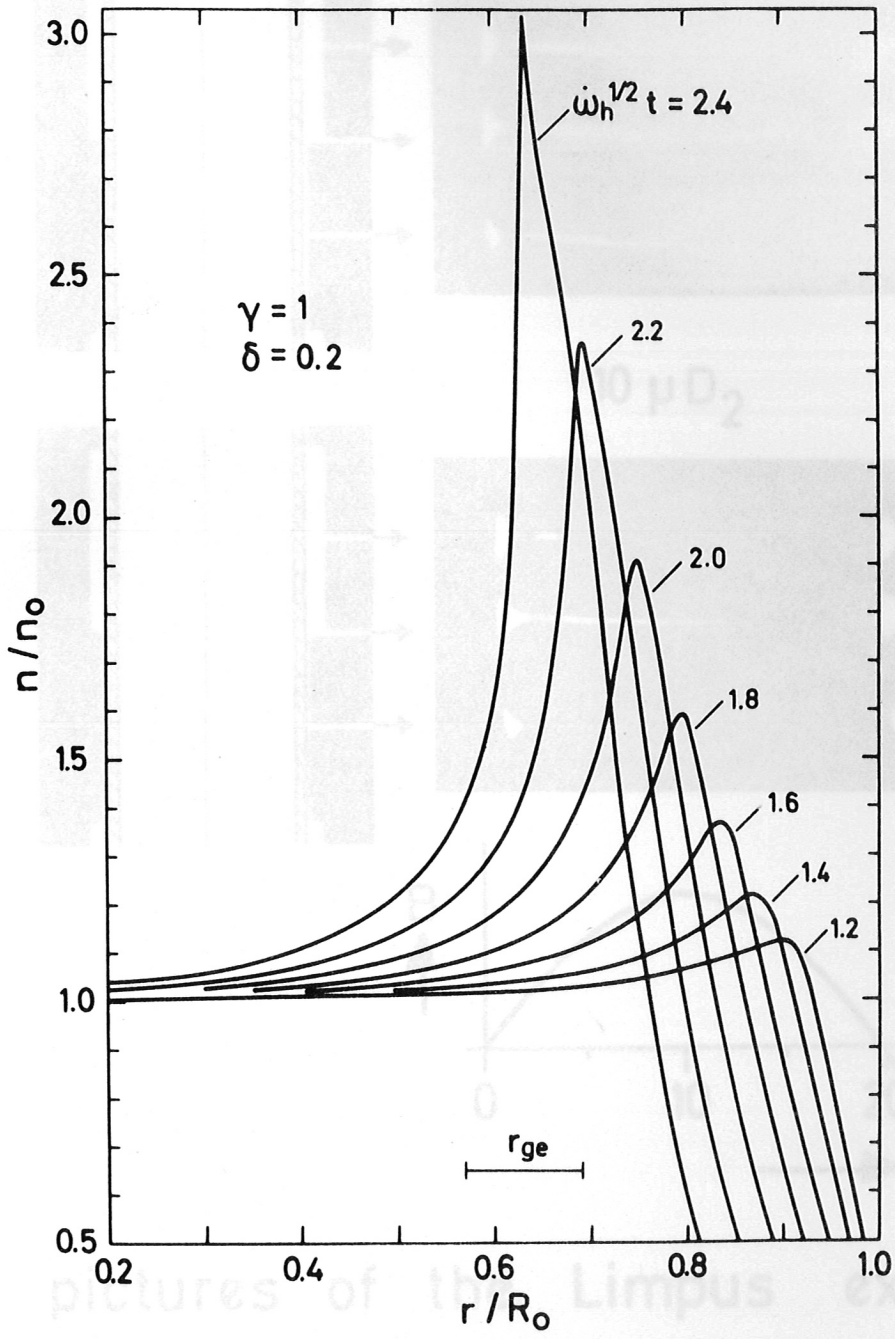

$B_0 = 0$

$$\dot{\omega}_h = \frac{e \cdot \dot{B}_a}{(m_i \cdot m_e)^{1/2}} \qquad \sigma = \frac{c}{\omega_{pe} \cdot R_0}$$

Fig. 22 Density profiles at various times

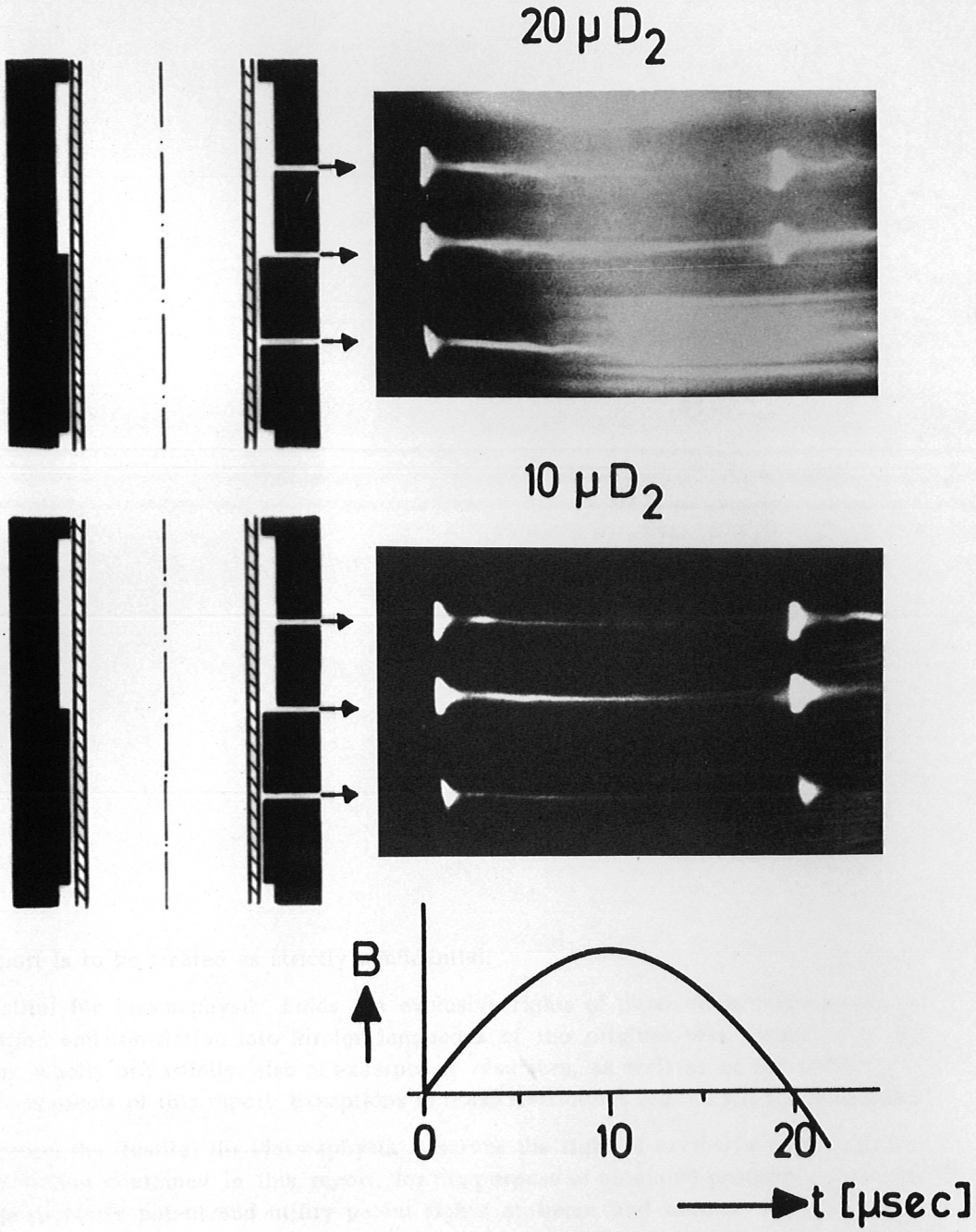

Fig. 23

Streak pictures of the Limpus experiment at two different initial pressures